  Journal of Hydroinformatics | 04.4 | 2002

Verification and application of a mathematical model for the assessment of the effect of guiding walls on the hydraulic efficiency of chlorination tanks

Anastasios I. Stamou

ABSTRACT

A mathematical model is applied to the tank of Kipseli in Athens, Greece, which is used for storage, balancing and emergency chlorination. A Flow-Through Curve (FTC) experiment is performed for the initial geometry of the tank. The shape and the characteristics of the FTC show a very poor hydraulic efficiency, with extensive short-circuiting, intense mixing and low detention times. To improve the hydraulic efficiency of the tank the use of four alternative arrangements of guiding walls is examined by the model. Prior to its application, the model is verified by comparing the predicted FTC with the experimental. A satisfactory agreement is observed between the calculated and the experimental curves. Then the model is applied to calculate the flow field and the FTC for the four arrangements. Calculations are compared and the arrangement which shows the highest hydraulic efficiency is proposed for construction.

Key words | chlorination tanks, Flow-Through Curve (FTC), hydraulic efficiency, mathematical models

Anastasios I. Stamou
Department of Civil Engineering,
National Technical University of Athens,
Iroon Polytechniou 5, 15780 Athens, Greece
Tel: +30 01 07722809;
Fax: +30 01 07722814;
E-mail: *stamou@central.ntua.gr*

INTRODUCTION

In water supply networks, storage tanks are commonly used for emergency chlorination. The chlorination efficiency, i.e. the removal of pathogenic bacteria, depends on the hydraulic (convective and diffusive) characteristics of the flow in the tanks. 'Parallel (or plug) flow' conditions are more favourable for chlorination than 'complete mixed' conditions (Falconer & Liu 1987). Thus, any modification made in the tanks, which drives the flow pattern closer to the 'parallel flow', such as the use of guiding walls, is expected to improve the hydraulic and the chlorination efficiency.

In existing tanks the effect of guiding walls on the flow field and on chlorination efficiency can be studied experimentally. However, the experimental determination of local flow velocities is a very difficult, expensive and time-consuming task; thus, in the majority of the practical cases it is not (or cannot be) performed. Alternatively, the Flow-Through Curve (FTC) can be experimentally determined and used to provide gross information on the hydraulic characteristics of the tanks. The experimental derivation of a FTC involves a simple tracer technique. A mass of tracer is injected instantaneously at the inlet of the tank and the resulting plot of the tracer concentration vs time at the outlet is the FTC. The FTC is essentially the probability density function (pdf) of the detention times in the tank. The shape of the FTC and its statistical characteristics provide information on the convective and the diffusive (dispersion) characteristics of the flow (Stamou & Noutsopoulos 1994).

In tanks, which are in the phase of design, the effect of guiding walls on the flow field can be studied with mathematical models. A mathematical model consists of a flow model and a process (or water quality) model. From the solution of the equations of the flow model the flow field is determined. Then the flow field is used as input to the process model, which consists of convection–diffusion equations for the concentrations of the process variables (e.g. chlorine and pathogens), to determine the fields of concentrations of the process variables and the efficiency of chlorination. A model can also be used for the simulation of a FTC experiment. FTC can be calculated from the solution of a non-steady tracer concentration convection–diffusion equation.

In the present work the commercial software package CFX-5 (AEA Technology 1999*a*, *b*) is applied to an existing water tank. Flow field and FTC calculations are performed for the initial geometry and four alternative arrangements of guiding walls, which are expected to improve the hydraulic efficiency of the tank. Firstly, the model is verified by comparison of the simulated FTC with the experimental one for the initial geometry of the tank. Then, the flow field and FTC calculations are compared for the four arrangements of guiding walls. The arrangement which shows the best hydraulic efficiency is proposed for construction.

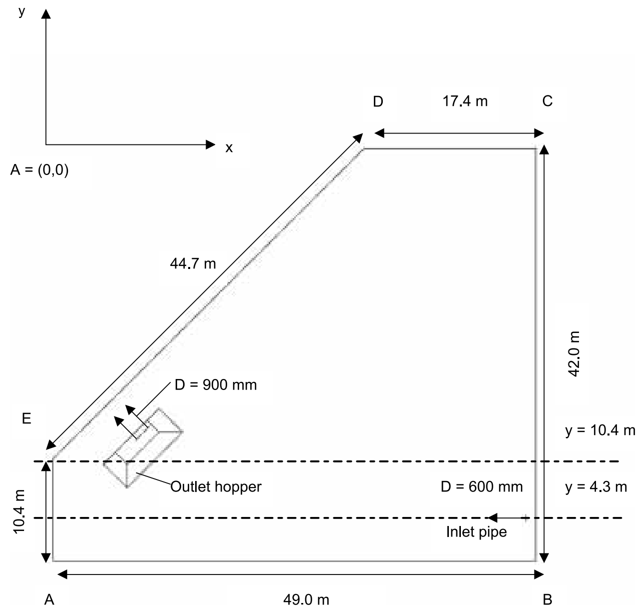

Figure 1 | Initial geometry of the tank.

EXPERIMENTAL

The water supply system of the greater area of Athens, Greece, includes 50 tanks with a total volume of approx. 200,000 m^3. The majority of these tanks have been designed and constructed 20–30 years ago for water storage or balancing purposes. Only recently, EYDAP SA, the company responsible for the water supply and sewerage systems of Athens, decided to upgrade the most important of these tanks, so they can be used for emergency disinfection. The procedure of upgrading includes:

1. identification of the tanks having poor hydraulic efficiency, by performing FTC experiments,
2. use of mathematical models to examine the effect of possible arrangements of guiding walls, which can be constructed easily, economically and without significant disruption of the operation,
3. comparison of the results of the model for all alternatives and selection of the arrangement which shows the best hydraulic efficiency, and
4. implementation of the proposed arrangement in the tanks.

This procedure has been applied to the tank of Kipseli, an important component of the water supply system of the greater area of Athens. In Figure 1, a simplified geometrical representation of the tank is shown. The water flows into the tank from a 600 mm inlet pipe, located in corner B of the tank (see Figure 1) and at a distance of 200 mm from the bottom. The flow exits the tank via two pipes (each of diameter 900 mm), placed in a hopper at the bottom of the tank, close to corner E. There are also 41 columns in the tank, with rectangular cross sections 0.5 m × 0.5 m (not shown in Figure 1).

Experimental determination of the FTC

A mass of sodium chlorine, $M_{in} = 316.0$ kg, has been injected for a relatively short time, $T_{in} = 3.0$ min (approximately 3% of the average theoretical detention time), into the inlet pipe of the tank. At the two outlet pipes, samples have been taken every 1 or 2 min, chlorine concentrations have been determined (using the Mohr method) and two FTC plots have been derived. The experiment had a duration of $T_{ex} = 343$ min and the recovery of the tracer was $R = 93.1\%$. Due to the mode of operation of the tank, the flow rate (Q) and the water depth (H) could not be kept constant, but varied from 20.60 to 51.20 $m^3\ min^{-1}$ and from 2.90 to 3.03 m, respectively. The average values of the flow rate and water

 Journal of Hydroinformatics | 04.4 | 2002

Table 1 | FTC characteristics

Indicator	Indicator	Initial geometry experiment	Initial geometry model	Modified geometry A	Modified geometry B	Modified geometry C	Modified geometry D
(1) Short circuiting	θ_0	0.02	0.02	0.04	0.18	0.12	0.12
	θ_{10}	0.04	0.047	0.21	0.39	0.28	0.41
(2) Mixing dispersion	θ_{75}–θ_{25}	1.05	1.11	0.94	0.74	0.88	0.64
	θ_{90}–θ_{10}	1.87	2.25	1.79	1.45	1.67	1.32
	θ_{90}/θ_{10}	45.75	46.87	9.62	4.77	7.06	4.26
	Var	0.33	0.32	0.22	0.12	0.17	0.12
(3) Fractions of PF	p	0.19	0.21	0.35	0.44	0.38	0.45
	1-p	0.81	0.79	0.65	0.56	0.62	0.55
	V_R^*	—	—	0.46	0.43	0.44	0.39
(4) Efficiency	θ_{max}	0.04	0.035	0.24	0.43	0.27	0.58
	θ_{50}	0.57	0.61	0.71	0.82	0.77	0.83

*The values of V_R have been determined graphically from the flow field plots.

depth are $Q = 45.05\ m^3\ min^{-1}$ and $H = 2.91$ m, respectively. Using these values, the theoretical detention time and the average tracer concentration are calculated as $T = 100.9$ min and $C_0 = 0.07\ kg\ m^{-3}$, respectively.

Calculation of FTCs and their characteristics

The normalised average FTC, $E(\theta)$, and the cumulative FTC, $F(\theta)$, are calculated following the procedure described in Stamou & Noutsopoulos (1994). In the average FTC, the tracer concentrations are normalised by C_0, the times by T, $\theta = t/T$, while the area below the FTC is equal to unity, after division by R.

Certain FTC characteristics can be used as 'indicators of the flow'. In the present work 10 characteristics are used, which are grouped into four broad categories of indicators: (1) short circuiting, (2) mixing–dispersion, (3) degree of PF (plug flow) and (4) efficiency. More specifically: (1) short-circuiting indicators are the initial arrival time (θ_0) and the time at which 10% of the tracer has passed the outlet (θ_{10}); (2) mixing indicators are measures of the width of the FTC. These are time differences (θ_{75}–θ_{25} and θ_{90}–θ_{10}), time ratios (θ_{90}/θ_{10}) and the (statistical) variance of $E(\theta)$, Var; (3) PF indicators attempt to establish effective fractions of the PF (p) and completely mixed conditions (1-p) regions according to the theory of Rebhun & Argaman (1965); (4) the characteristic times, which are used as indicators of the efficiency, are the most probable time (θ_{max}) and the time at which 50% of the tracer has passed (θ_{50}).

In Table 1 the characteristics of the experimental FTC are shown. Since only one FTC experiment was conducted, care should be taken in the interpretation of the FTC and its characteristics. A theoretical method is described in Adams & Stamou (1988), according to which the statistical uncertainly for all characteristics was calculated to be less than 5%, except for the characteristics near the peak, where the error was approximately 10%.

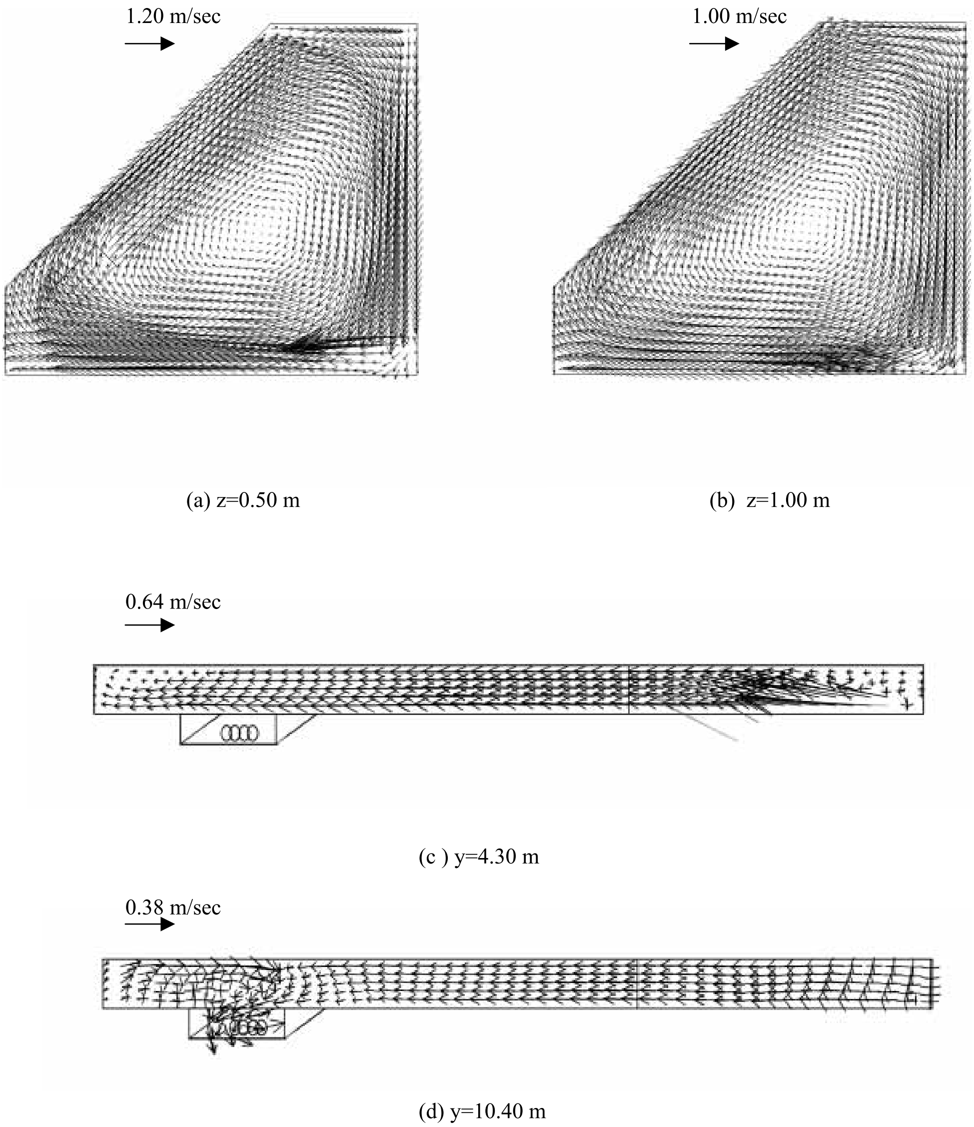

Figure 2 | Calculated flow field for the initial geometry.

Similar figures have been found by performing a statistical survey on a series of 12 FTCs obtained under the same conditions (see also Stamou & Noutsopoulos 1994).

MODEL CALCULATIONS

The mathematical model

General features

Calculations have been performed with CFX-5 (AEA Technology 1999*a*, *b*). The 3D steady-state flow field is determined from the solution of the equations of continuity and momentum, incorporating the standard k–ε turbulence model (Rodi 1980). CFX-5 employs unstructured numerical grids, which permit a very accurate representation of the boundaries. The algebraic equations are derived using second-order spatial discretisation schemes and are solved in a coupled fashion with a fast and robust procedure. The FTC is calculated from the solution of a non-steady tracer concentration convection–diffusion equation using the calculated steady-state flow field as

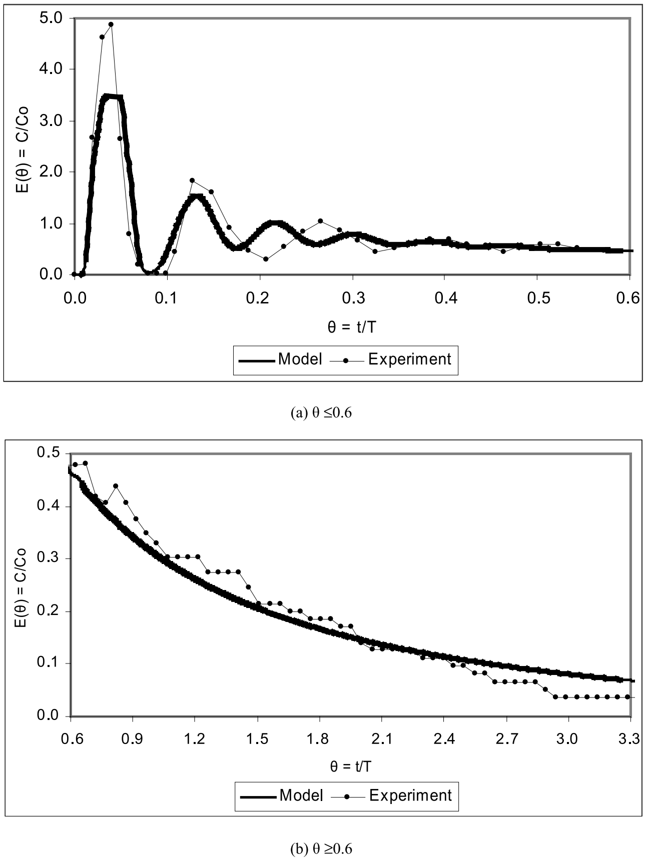

Figure 3 | Calculated vs experimental FTC for the initial geometry.

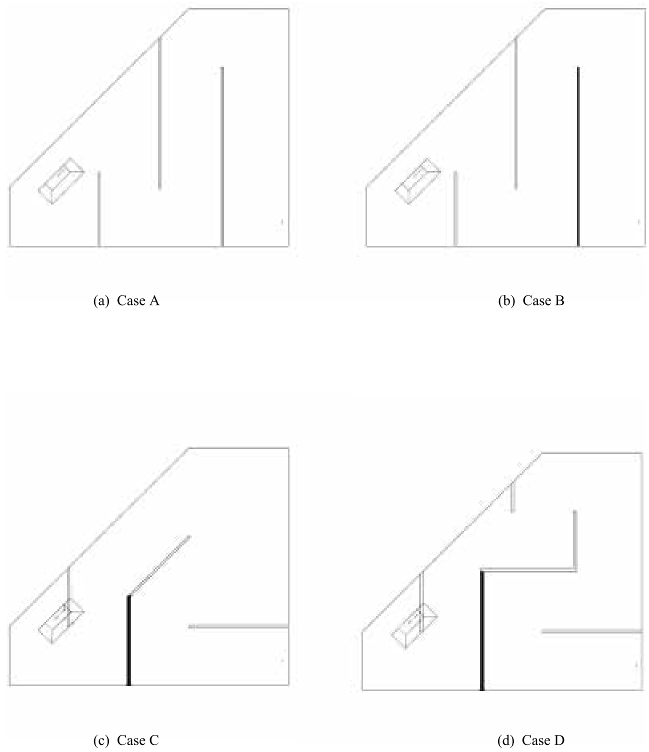

Figure 4 | Approximated modified geometries of the tank with guiding walls.

input. For more information on CFX-5, readers are referred to AEA Technology (1999*a*, *b*) and Wright & Hargreaves (2001).

Boundary conditions and numerical grid

Boundary conditions are defined at the borders of the computation domain. At the inlet pipe a parallel flow is imposed, with uniform horizontal velocity and vertical velocity equal to zero. The turbulent energy (k) and its dissipation rate (ε) are assumed to be uniform, with values corresponding to an eddy viscosity at the inlet approximately 100 times the molecular viscosity of water. The tracer concentration, C, is assumed to be uniformly distributed at the inlet. At the outlet pipes the pressure is specified and the vertical gradients of k, ε and C are set equal to zero. The free surface is treated as a symmetry plane using the rigid-lid approximation; accordingly, the normal velocity component and the normal gradients of all other variables are set to zero. At rigid walls, the standard wall function approach is applied, which relates the shear stress at the wall to the cell node velocity component parallel to the wall. All velocity components and the fluxes of C are set to zero. The guiding walls are treated as wall boundaries. The 41 columns of the tank are ignored, because they are not expected to noticeably affect the flow field, due to their small size. Furthermore, their modelling would have resulted in a very large grid size.

In the simulation of the FTC, the injection of the tracer is represented by a square step input of duration equal to the injection time (T_{in}).

The computational grid consists of 475,000 tetrahedral elements with grid refinement in the inlet and outlet regions. The size of the grid has been chosen after a series of preliminary calculations to ensure grid-independent calculations.

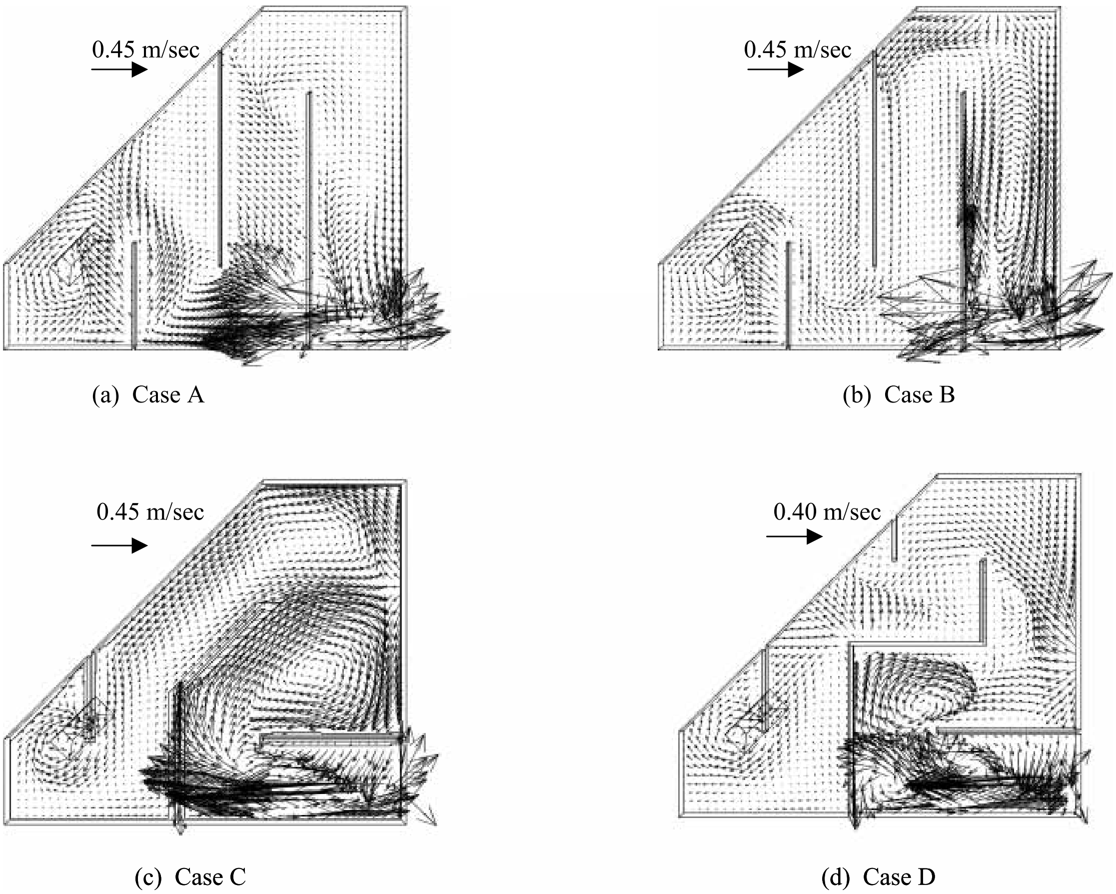

Figure 5 | Calculated flow fields for cases A, B, C and D (z=0.10 m).

Characteristics of the calculations

A Pentium II PC operating at 600 MHz was used in the computations. For steady state flow field calculations 500 iterations were required for convergence and the real computation time was 29 h. FTC calculations have been performed with a variable time step, dt, ranging from 4 s for θ values less than 0.5 to 40 s for θ values greater than 0.5. For a total simulation time of 3.3T the real computation time was 110 h.

Initial geometry—verification of the model

Flow field calculations

In Figure 2 the calculated velocity vectors on horizontal planes at levels $z = 0.50$ m (coinciding with the axis of the inlet pipe, Figure 2(a)) and $z = 1.00$ m (Figure 2(b)) and at vertical cross sections of constant $y = 4.30$ m (Figure 2(c)) and $y = 10.40$ m (Figure 2(d)) are shown.

The main characteristic of the flow field is a massive, clockwise recirculation region, which occupies almost 95% of the volume of the tank. Due to the formation of this recirculation region, a significant part of the flow exits the tank via a short-circuiting route parallel to walls BA and AE (see Figures 1, 2(a) and 2(b)). A second, very small recirculation region is formed over the exit hopper (see Figures 2(c) and 2(d)).

High flow velocities (1.5–2.5 m s^{-1}) are observed in the inlet region and in the perimeter of the large recirculation region, close to the walls (approx. 0.5 m s^{-1}). Very low velocities are found in the centre of the recirculation region, where settling of suspended matter is expected to

 Journal of Hydroinformatics | 04.4 | 2002

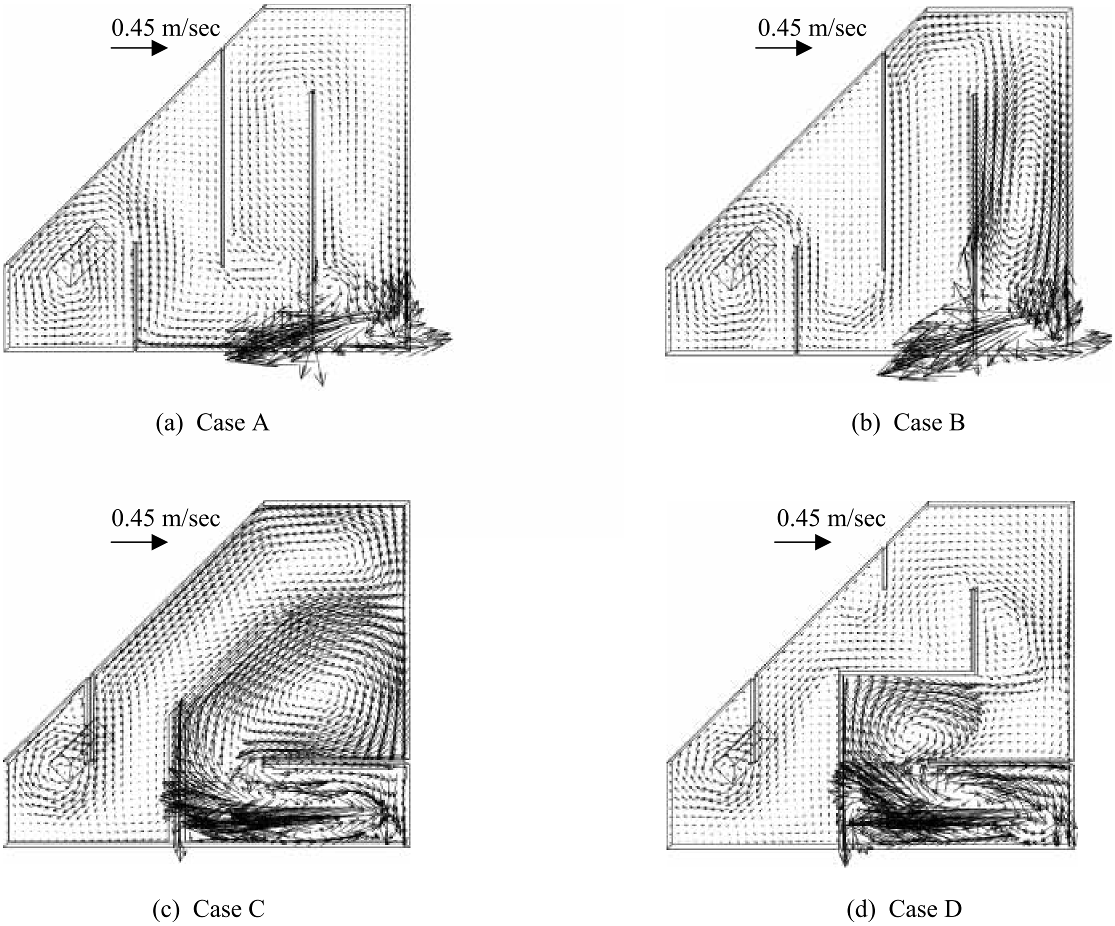

Figure 6 | Calculated flow fields for cases A, B, C and D ($z = 1.00$ m).

occur. Indeed, during the evacuation of the tank for maintenance (cleaning, etc.), significant quantities of deposited matter have been observed in this region.

FTC calculation–verification of the model

In Figure 3 the computed FTC, $E(\theta)$, is shown together with the experimental curve. There is a satisfactory agreement between the two curves, taking into consideration that (i) only one FTC experiment has been performed and (ii) the flow and the water depth were not constant during the FTC experiment.

The FTCs can be divided into three parts:

1. $\theta = 0.02$–0.08. The first part of the computed FTC is a relatively symmetrical curve with a rising and a falling part. This part represents the volume of tracer, $F(0.08) = 15\%$, reaching the outlet ($\theta_0 = 0.02$ and $\theta_{10} = 0.05$) via the short-circuiting route. The maximum value of the FTC, $E(\theta_{\max}) = 3.5$ is observed at $\theta_{\max} = 0.047$. There is a satisfactory agreement of the computed FTC with the experimental. The corresponding experimental values are: $\theta_0 = 0.02$, $\theta_{10} = 0.04$, $F(0.08) = 16\%$, $E(\theta_{\max}) = 4.9$ and $\theta_{\max} = 0.04$.
2. $\theta = 0.08$–0.40. The second part represents the volume of tracer, which exits the tank after flowing three times in the large recirculation region. The computed FTC shows a periodic behaviour with three local maximum values, which decrease with time (Figure 3(a)). The period, which is determined

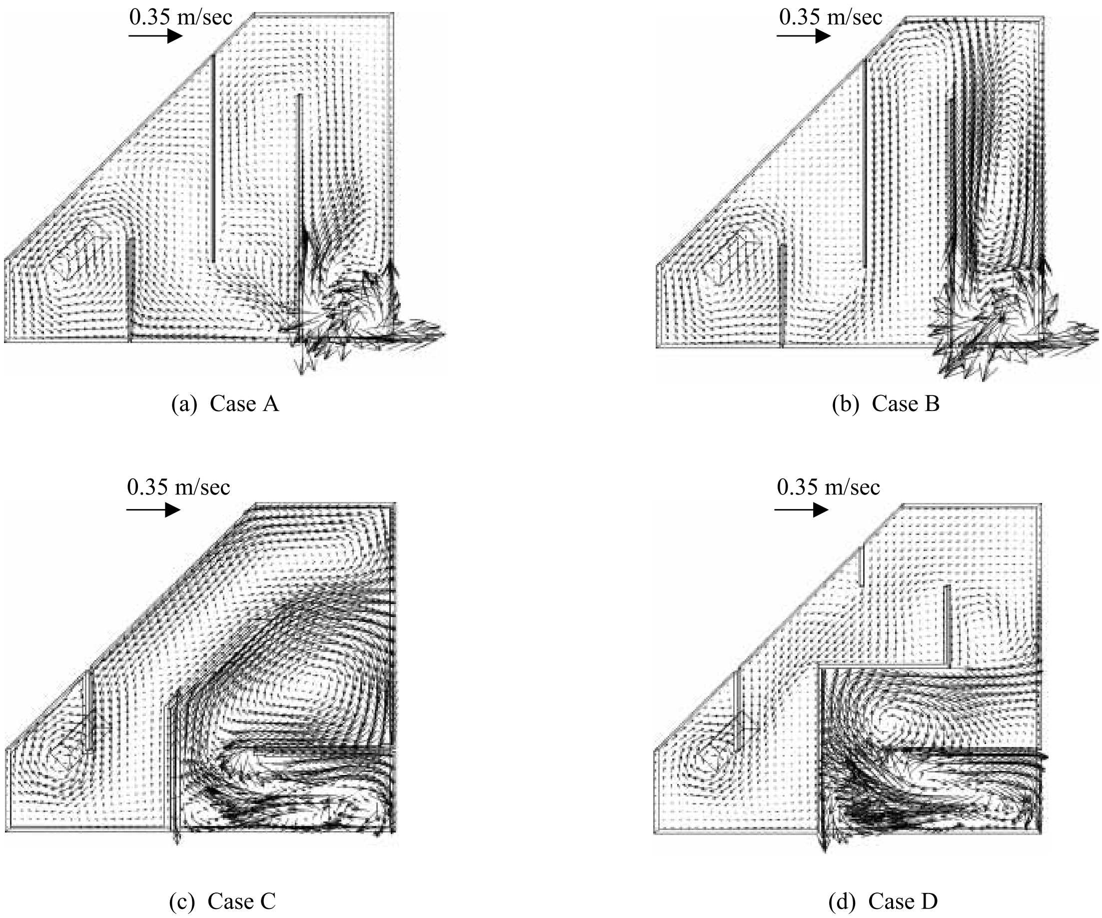

Figure 7 | Calculated flow fields for cases A, B, C and D (z= 2.00 m).

to be equal to 8.9 min or $0.09T$, is eventually the time needed for the tracer to complete a passage in the large recirculation region. The experimental FTC shows a similar behaviour with three maximum values, but with a longer period (12 min or $0.12T$) and a faster decay of the maximum values. These differences suggest that there is a higher level of mixing in the main part of the real tank than for the one in the model. This behaviour can be partly attributed to the additional turbulence created by the 41 columns in the tank, which are not taken into account in the model. Due to the higher levels of turbulence, the second part of the experimental FTC ends later than the computed, at approx. $\theta = 0.55$.

3. $\theta > 0.40$ (or 0.55 for the experimental curve). The last part of the FTC represents the volume of the tracer, which exits the tank after remaining in the relatively slow central parts of the recirculation regions in the tank. This volume is calculated to be equal to 38%, a value similar to the experimental value, 36%. The two curves almost coincide (see Figure 3(b)) and have an exponential shape, which resembles the completely mixed theoretical FTC.

Use of guiding walls—application of the model—discussion

Calculations have been performed for the four alternative arrangements of guiding walls shown in Figure 4, which

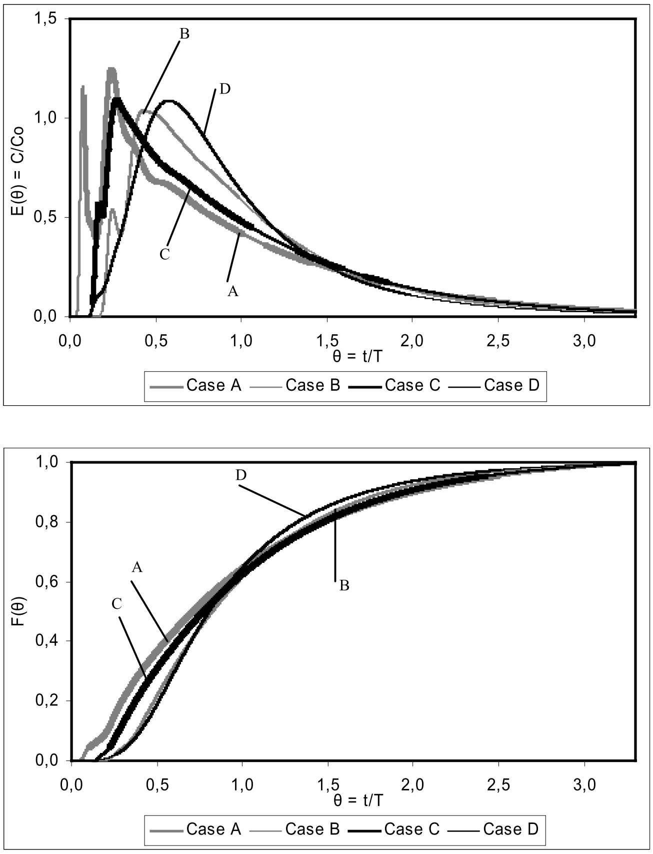

Figure 8 | Calculated FTCs for cases A, B, C and D.

are characterised as cases A, B, C and D. The guiding walls extend from the water surface to a distance $z=0.15$ m from the bottom, to facilitate the cleaning of the tank, with the exception of the guiding walls facing the inlet pipe in cases B, C and D (shown in Figure 4 by thick lines), which extend to the bottom to prevent short-circuiting.

In Figures 5, 6 and 7 the calculated velocity vectors are shown for cases A, B, C and D, at horizontal planes $z=0.10$ m, 1.00 m and 2.00 m, respectively. These 2D patterns provide a clear view of the main flow characteristics, despite the 3D nature of the flow near the inlet and outlet regions of the tank. A similar behavior has been observed by Shiono & Texeira (2000), who performed velocity measurements in a baffled contact tank and observed a highly 3D flow in the inlet and outlet regions, tending to 2D in the remaining compartments of the tank.

In Figure 8 the calculated FTCs for all arrangements, including the initial geometry, are shown. In Table 1 the corresponding characteristics of the FTCs are quoted.

Based on Figures 5–8 and Table 1 the following remarks can be made:

1. Short-circuiting. In case A, part of the incoming flow passes under the guiding walls and exits the tank via a short-circuiting route (see Figure 5(a)). From the flow field results, the length of this route is calculated to be equal to 89.5 m. This short-circuiting is verified by the very small values of $\theta_0=0.04$ and $\theta_{10}=0.21$. In cases B, C and D the guiding wall facing the inlet pipe extends to the bottom, resulting in a significant increase of the length of the shortest route to the exit, which is calculated to be equal to 155.6 m, 142.8 and 140.7 m, respectively. These values are consistent with the θ_0 values, which are 0.18, 0.12 and 0.12, respectively, showing that case B exhibits the latest initial arrival of tracer in the exit. The values of θ_{10} show that cases B and D show the lowest short-circuiting.
2. Mixing. In all arrangements 4–6 recirculation regions are formed, where large scale mixing occurs. The values of the total volumes of these regions (V_R) have been determined graphically using the 2D velocity plots, and are shown in Table 1 together with the values of mixing characteristics $1-p$, θ_{75}–θ_{25}, θ_{90}–θ_{10}, θ_{90}/θ_{10} and Var of the FTC. The V_R values are approximately 70% of the values of the regions with completely mixed flow $(1-p)$, determined according to the theory of Rebhun & Argaman (1965). The values of all mixing characteristics show a reduction of the degree of mixing in the order: A–C–B–D, i.e. D has the lowest degree of mixing.
3. Degree of PF. The calculation of plug flow fractions (p) shows that the order of the increase of p is the same as the order of the reduction of mixing. The largest value of p is observed for case D.
4. Detention times. As expected, the highest values of θ_{max} and θ_{50} are observed for case D, which shows the highest fraction of PF conditions.

CONCLUSIONS

The following conclusions are drawn:

1. The poor hydraulic efficiency of the tank of Kipseli, an existing tank used for emergency chlorination, can be significantly improved with the use of guiding walls.
2. A mathematical model is used to calculate the flow field and the FTC for the initial geometry, i.e. without guiding walls, and four alternative arrangements of guiding walls (cases A, B, C and D). Prior to its application, the model is verified by comparison of the computed FTC with an experimental one for the initial geometry of the tank. A satisfactory agreement is observed between the calculated and the experimental curve.
3. From comparison of the flow fields and the FTC results, the arrangement of guiding walls of case D creates a flow pattern, which is closer to the 'parallel flow' than the other arrangements. Therefore, case D shows the highest hydraulic efficiency and subsequently the highest chlorination efficiency, and it is proposed for construction.
4. The present procedure can be applied to any tank, to investigate the effect of possible geometrical modifications on the hydraulic efficiency of the tank, prior to their implementation in the real tank.

ACKNOWLEDGEMENTS

The author would like to thank EYDAP SA for the financial support, the personnel of EYDAP SA for providing the required information and data (Dr Ph. Tzoumerkas, Mr S. Georgiades and Mrs S. Kanelopoulou), Dr G. Theodoridis for the setup of the computer code, Mr I. Katsiris for performing a series of computations and KALAS SA (Mr K. Kalamarakis and Mrs S. Zonorou) for the provision of the required quantities of salt for the performance of the FTC experiments.

REFERENCES

Adams, E. W. & Stamou, A. I. 1988 A study of the flow in a two-dimensional model settling tank: slot inlet, SFB210/E/40, University of Karlsruhe.

AEA Technology 1999*a* *CFX-5.3 User Guide*, 8.19, Harwell, Didcot, UK.

AEA Technology 1999*b* *CFX User Conference, Friedrichshafen, Germany*.

Falconer, R. A. & Liu, S. Q. 1987 Mathematical model study of plug flow in a chlorine contact tank. *J. Inst. Wat. Environ. Mngt.* **1**(3), 279–290.

Rebhun, M. & Argaman, Y. 1965 Evaluation of hydraulic efficiency of sedimentation basins. *J. Sanit. Engng. Div., ASCE* **91**, 37–45.

Rodi, W. 1980 *Turbulence Models and Their Application in Hydraulics—A State of the Art Review*. IAHR, Delft, The Netherlands.

Shiono, K. & Texeira, E. C. 2000 Turbulent characteristics in a baffled contact tank. *J. Hydraul. Res.* **38**(6), 403–416.

Stamou, A. I. & Noutsopoulos, G. 1994 Evaluating the effect of inlet arrangement in settling tanks using the hydraulic efficiency diagram. *Water SA* **20**(1), 77–83.

Wright, N. G. & Hargreaves, D. M. 2001 The use of CFD in the evaluation of UV treatment systems. *J. Hydroinformatics* **3**(2), 59–70.